

# Cortical hyperpolarization-activated depolarizing current takes part in the generation of focal paroxysmal activities

Igor Timofeev\*<sup>†</sup>, Maxim Bazhenov<sup>‡</sup>, Terrence Sejnowski<sup>§5</sup>, and Mircea Steriade\*

\*Laboratory of Neurophysiology, Faculty of Medicine, Laval University, Quebec City, QC, Canada G1K 7P4; <sup>‡</sup>Howard Hughes Medical Institute, The Salk Institute, Computational Neurobiology Laboratory, 10010 North Torrey Pines Road, La Jolla, CA 92037; and <sup>§</sup>Department of Biology, University of California, La Jolla, CA 92093

Communicated by Rodolfo R. Llinás, New York University Medical Center, New York, NY, May 1, 2002 (received for review December 26, 2001)

**During paroxysmal neocortical oscillations, sudden depolarization leading to the next cycle occurs when the majority of cortical neurons are hyperpolarized. Both the  $\text{Ca}^{2+}$ -dependent  $\text{K}^+$  currents ( $I_{\text{K}(\text{Ca})}$ ) and disfacilitation play critical roles in the generation of hyperpolarizing potentials. *In vivo* experiments and computational models are used here to investigate whether the hyperpolarization-activated depolarizing current ( $I_h$ ) in cortical neurons also contributes to the generation of paroxysmal onsets. Hyperpolarizing current pulses revealed a depolarizing sag in  $\approx 20\%$  of cortical neurons. Intracellular recordings from glial cells indirectly indicated an increase in extracellular potassium concentration ( $[\text{K}^+]_o$ ) during paroxysmal activities, leading to a positive shift in the reversal potential of  $\text{K}^+$ -mediated currents, including  $I_h$ . In the paroxysmal neocortex,  $\approx 20\%$  of neurons show repolarizing potentials originating from hyperpolarizations associated with depth-electroencephalogram positive waves of spike-wave complexes. The onset of these repolarizing potentials corresponds to maximal  $[\text{K}^+]_o$  as estimated from dual simultaneous impalements from neurons and glial cells. Computational models showed how, after the increased  $[\text{K}^+]_o$ , the interplay between  $I_h$ ,  $I_{\text{K}(\text{Ca})}$ , and a persistent  $\text{Na}^+$  current,  $I_{\text{Na}(\text{P})}$ , could organize paroxysmal oscillations at a frequency of 2–3 Hz.**

The depolarizing and hyperpolarizing phases of neocortical paroxysmal activities during electrographic seizures resemble the up and down components of the slow sleep oscillation (1). Sudden depolarization leading to the next paroxysmal cycle starts when the overwhelming majority of neurons are hyperpolarized. The generation of hyperpolarizing potentials involves both  $\text{Ca}^{2+}$ -dependent  $\text{K}^+$  currents,  $I_{\text{K}(\text{Ca})}$ , and the disfacilitation that results from the absence of synaptic activities in the network (2, 3). The increase of extracellular potassium concentration ( $[\text{K}^+]_o$ ) during epileptogenesis (4) results in cellular depolarization, increased excitability, and decreased inhibition (5, 6) as well as conversion of some regular-spiking neurons to intrinsically bursting ones (7, 8). The impact of bursts produced by intrinsically bursting neurons on postsynaptic cells is greater than the impact of single spikes (9), indicating that this may be one of the mechanisms underlying overexcitation in the paroxysmal neocortex. The increased  $[\text{K}^+]_o$  shifts the reversal potentials for different  $\text{K}^+$ -mediated currents and, in particular, increases the reversal potential and maximal conductance of the hyperpolarization-activated cation current ( $I_h$ ) (10). Almost 60% of cortical neurons display low-frequency (1–3 Hz) resonance mediated via  $I_h$  and enhanced by the persistent  $\text{Na}^+$  current,  $I_{\text{Na}(\text{P})}$  (11, 12).

Here we show that  $\approx 20\%$  of neocortical neurons display a depolarizing sag after the application of hyperpolarizing current pulses. In the paroxysmal neocortex, after the end of paroxysmal depolarizing shifts (PDSs) the same proportion of neurons show repolarizing potentials originating from hyperpolarizations associated with focal depth electroencephalogram (EEG)-positive “wave” components of spike-wave (SW) complexes. The onset of these repolarizing potentials followed the maximal  $[\text{K}^+]_o$  as estimated from dual simultaneous impalements from neurons

and glial cells. Using a computational model, we found that a  $[\text{K}^+]_o$ -mediated increase of  $I_h$  could initiate 2–3-Hz activity in a model of the cortical network.

## Materials and Methods

*In vivo* experiments were carried out on 35 adult cats anesthetized with ketamine and xylazine (10–15 and 2–3 mg/kg i.m., respectively). The EEG was monitored continuously during the experiments to maintain a deep level of anesthesia and additional doses of anesthetic were given at the slightest tendency toward an activated EEG pattern. In addition, all pressure points and tissues to be incised were infiltrated with lidocaine. The cats were paralyzed with gallamine triethiodide and ventilated artificially to an end-tidal  $\text{CO}_2$  of 3.5–3.8%. The heartbeat was monitored and kept constant (90–110 beats per min). Body temperature was maintained at 37–39°C. Glucose saline (5% glucose, 10 ml i.p.) was given every 3–4 h during experiments, which lasted for 8–14 h.

Local field-potential (depth-EEG) recordings were obtained and stimulation was delivered by means of bipolar coaxial macroelectrodes inserted in the suprasylvian area 5, suprasylvian area 7, and/or precruciate area 4. The micropipettes for intracellular recordings in the cortex were placed in the vicinity of at least one EEG electrode. All pipettes also contained 1.5% of Neurobiotin. The stability of intracellular recordings was ensured by cisternal drainage, bilateral pneumothorax, hip suspension, and by filling the hole made in the skull with a 4% solution of agar. A microsyringe containing 0.2 mM bicuculline was inserted in area 4. Intracellular recordings were performed in suprasylvian areas 5 and 7 to avoid the direct influence of bicuculline on recorded neurons. At the end of experiments, the cats were given a lethal dose of pentobarbitone and perfused intracardially with physiological saline followed by 4% formaldehyde and 1% glutaraldehyde.

A one-dimensional, two-layer network model of cortical excitatory (PY) and inhibitory (IN) cells with local connectivity was simulated. In most simulations, the model included 20 PY and 20 IN cells. Larger models were also tested. Each PY cell made  $\alpha$ -amino-3-hydroxy-5-methyl-4-isoxazolepropionic acid (AMPA)-mediated connections with all other cells within a fixed radius of four cells, and each IN cell made  $\gamma$ -aminobutyric acid type A ( $\text{GABA}_A$ )-mediated connections with PY cells within the same radius. A simple model of synaptic plasticity (13) was used to describe short-term depression of PY and IN synaptic connections (14). All AMPA- and  $\text{GABA}_A$ -mediated synapses were modeled by first-order activation schemes, and the expressions for the kinetics are given elsewhere (15). Intrinsic properties of

Abbreviations:  $[\text{K}^+]_o$ , extracellular potassium concentration;  $I_{\text{K}(\text{Ca})}$ ,  $\text{Ca}^{2+}$ -dependent  $\text{K}^+$  current;  $I_h$ , hyperpolarization-activated depolarizing current;  $I_{\text{Na}(\text{P})}$ , persistent  $\text{Na}^+$  current; PDS, paroxysmal depolarizing shift; EEG, electroencephalogram; SW, spike wave; PY, excitatory; IN, inhibitory; AMPA,  $\alpha$ -amino-3-hydroxy-5-methyl-4-isoxazolepropionic acid.

<sup>†</sup>To whom reprint requests should be addressed. E-mail: Igor.Timofeev@phs.ulaval.ca.

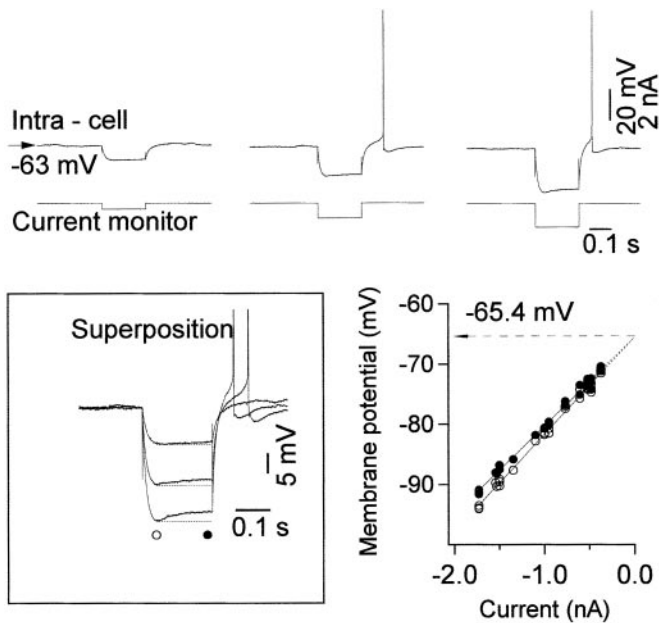


**Fig. 1.** The depolarizing sag in cortical neurons in response to intracellular application of hyperpolarizing current pulses. (*Upper*) Examples of responses of neurons to different intensities of hyperpolarizing current pulses in barbiturate-anesthetized cats during periods virtually free of spontaneous synaptic activities. (*Bottom Left*) Superposition of responses illustrated in *Upper*. (*Bottom Right*) Voltage-current relations for maximal hyperpolarization (○) and hyperpolarizing sag (●).

cortical neurons were modeled as described in a previous paper (16), with an  $I_{Na(P)}$  (17) and  $I_h$  (10, 12) added to the model. The  $I_{Na(P)}$  and  $I_h$  were described as follows:  $I_{Na(P)} = g_{Na(P)} m(v - 50)$ ,  $dm/dt = (m_\infty - m)/0.2$ ,  $m_\infty = 0.02/\{1 + \exp[-(v + 42)/5]\}$  (18) and  $I_h = g_h (0.8m_1 + 0.2m_2)(v + 40)$ ,  $dm_i/dt = -(m_\infty - m_i)/\tau_i$ ,  $m_\infty = 1/\{1 + \exp[(v + 82)/7]\}$ ,  $\tau_1 = 38$  ms,  $\tau_2 = 319$  ms (10).

## Results

We recorded activities from 196 neocortical neurons and intracellular activities from 17 presumed glial cells; four dual simultaneous recordings were obtained from neuron and glial pairs located in deep and superficial layers of areas 5 and 7. In the experiments described below, seizures were elicited by small infusions of bicuculline (0.2 mM) to a remote location in area 4. A primary paroxysmal focus occurred at the place of infusion, and after 30–60 min a secondary paroxysmal focus was usually induced in other cortical areas. Because only a small amount of bicuculline was infused in area 4, the inhibition in the secondary foci was not affected directly; presumably, the seizures were initiated in secondary foci because of paroxysmal activities in the primary focus. In some animals, the field-potential recordings revealed paroxysmal activities at the site of bicuculline injection immediately, but 2–3 h later the paroxysmal activity disappeared at the site of injection (data not shown). Intracellular recordings from pairs of neurons separated by less than 0.5 mm were performed in secondary foci. Under these conditions, neurons recorded simultaneously with two pipettes displayed a high level of synchrony, and the intracellular traces were extremely similar for both neurons (data not shown).

Neurons were classified as regular-spiking, fast rhythmic-bursting, intrinsically bursting, and fast-spiking (19–21) according to their responses to depolarizing and hyperpolarizing current pulses. During periods with relatively low levels of synaptic activity, in particular during depth-EEG positive waves of the slow oscillation, 20% of cortical neurons displayed depolarizing

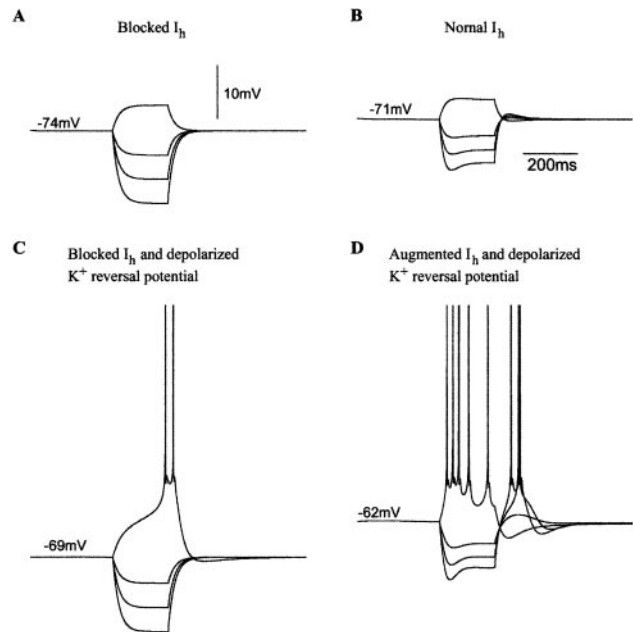


**Fig. 2.** Model—effects of  $K^+$ -dependent  $I_h$  modulation in PY response. An isolated PY cell was stimulated by 200-ms DC pulses (two positive and three negative pulses). (A)  $I_h$  is absent, and the reversal potential for  $K_{leak}$  is  $-75$  mV. (B) Weak  $I_h$  with reversal potential  $-50$  mV. (C)  $I_h$  is absent, and the reversal potential for  $K_{leak}$  is  $-70$  mV. (D) Strong  $I_h$  with a reversal potential of  $-30$  mV and maximal conductance at 200% of the example shown in B; the reversal potential for  $K_{leak}$  is  $-70$  mV.

sags after application of hyperpolarizing current pulses (Fig. 1), which probably was caused by activation of  $I_h$  (22). The depolarizing sag disappeared at voltages close to the baseline membrane potential (see the plot in Fig. 1) and was activated constantly at hyperpolarized levels. In most neurons, the offset of current pulse produced a rebound depolarization and firing.

We compared the response properties of neurons *in vivo* with those in a computation model of the cortex. In a model of an isolated cortical PY neuron (Fig. 2), the resting membrane potential was  $\approx -74$  mV without  $I_h$ , and no intrinsic currents were activated significantly during DC stimulation (Fig. 2A). When  $I_h$  current was included in the dendritic compartment of PY neuron, the soma was depolarized by  $\approx 3$  mV. A typical  $I_h$  depolarizing sag and rebound depolarization were observed in response to hyperpolarizing pulses (Fig. 2B). When the reversal potential for  $K^+$  leak current was depolarized by 5 mV and  $I_h$  was blocked (Fig. 2C), the cell depolarized to  $-69$  mV, and DC-evoked depolarization (as in Fig. 2A and B) was sufficient to activate  $I_{Na(P)}$ , leading to cell firing. To model the effects of increased extracellular  $K^+$  concentration, the reversal potentials for both the  $K^+$  leak current and  $I_h$  were depolarized simultaneously, and the maximal conductance for  $I_h$  was increased by 100% (10), producing a total depolarization of  $\approx 12$  mV at rest (Fig. 2D). Under these conditions, the depolarizing pulse evoked a tonic response with strong spike adaptation, and negative DC pulses produced rebound depolarization that was sufficient to generate a single  $Na^+$  spike or burst of spikes. The increased excitability of PY neurons after an increase of extracellular  $K^+$  contributes to the generation of paroxysmal synchronous oscillations in the network model.

We studied the intracellular activities of 157 cortical neurons from areas 5 and 7 during seizures that were initiated by infusions of small amounts of bicuculline into the remote area 4. In most neurons, sequences of PDSs were followed by a progressive hyperpolarization that reached its maximum just before

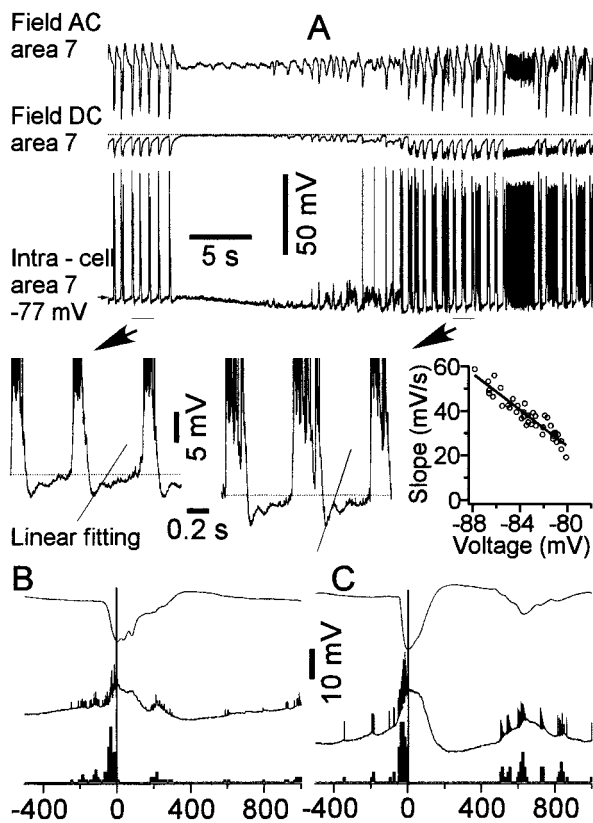


**Fig. 3.** Slowly repolarizing potential during the wave component of SW seizure. AC and DC field-potential and intracellular recordings from area 7. Seizures were induced by infusion of bicuculline into distantly located area 4. The neuron was hyperpolarized immediately after PDSs. This hyperpolarization resulted in an activation of slow neuronal depolarization. One possible candidate for such depolarizing sag at hyperpolarized levels is  $I_h$ . The plot shows the dependency of slope of linear fitting during the first 100 ms of depolarizing sag as a function of the membrane voltage. *B* and *C* show wave-triggered averages for EEG and two different neurons revealing the  $I_h$  component as well as their perievent firing histogram. The peak of EEG-depth negativity was taken as zero time for averages.

the onset of the next paroxysmal cycle. In those neurons, the next cycle appeared as a sudden depolarization. What triggered those PDSs? Of 157 neurons recorded during seizures, in 29 neurons the maximal hyperpolarization was achieved a few milliseconds after the previous PDSs, and thereafter those neurons progres-

sively revealed repolarizing potentials, which in 16 of them led to action potentials before the occurrence of the next PDS (Fig. 3). In those neurons, the time by which action potentials preceded the onset of PDS varied from 10 to 100 ms (Fig. 3 *B* and *C*), with an average of  $23 \pm 9$  ms. Those repolarizing potentials displayed properties similar to the  $I_h$ -mediated depolarizing sags (compare with Fig. 1); that is, the stronger the membrane potential hyperpolarization caused by spontaneous factors or direct injection of hyperpolarizing current, the larger the increase in the amplitude of depolarizing sags. To estimate the voltage dependency of  $I_h$ , we performed a linear fitting for 100-ms segments starting from maximal hyperpolarization achieved by a neuron after each consecutive PDS. Then, we plotted the slope of the linear fitting against voltage, and the slope approached zero values near the level of membrane potential (Fig. 3). All the neurons that revealed depolarizing sag during seizures were tested with hyperpolarizing current pulses, which uncovered depolarizing sag, thus suggesting that  $I_h$  in these neurons can contribute to repolarizing responses during seizures, leading to the next paroxysmal cycles. None of the neurons that did not reveal depolarizing sags during the EEG wave component of seizures fired before the onset of PDS, which was estimated from EEG recordings in the vicinity of intracellularly recorded neurons (data not shown).

In simultaneous intracellular recordings from neurons and glial cells (Fig. 4), the sudden onset of seizures was characterized by depolarization in both cells. We identified four different components of a paroxysmal cycle. The onset of PDS in the neuron was accompanied by a dramatic reduction in spike amplitude (1 in Fig. 4) and was followed by a plateau potential (2). Quite often but not necessarily always, the neuronal depolarization was followed by polyspike discharges (3). The paroxysmal cycle was terminated by neuronal hyperpolarization (4), corresponding to the depth-EEG positive wave. In 20% of cortical neurons, the hyperpolarization was relatively brief and was followed by a steady depolarizing potential leading to spikes, which preceded the onset of the next PDS (Figs. 3 and 4). In all cortical neurons recorded during seizures, at least the early part of depth-EEG positivity was accompanied by neuronal silence. An absence of neuronal firing during SW complexes also has been reported for the overwhelming majority of thalamocortical neurons (23–25), a major external input to cortex. Thus, the steady depolarizing potential in 20% of neurons most likely originated from intrinsic neuronal properties and not synaptic activities from other neuronal elements.

In nearby neuron-glia recordings, the neuronal firing always preceded by several milliseconds (see crosscorrelogram in Fig. 4) any detectable events in glial cells. Glial elements displayed

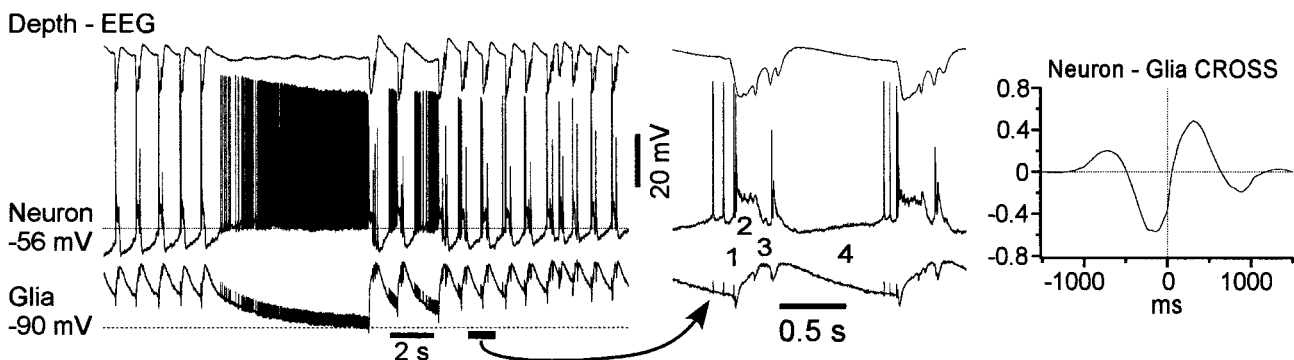


**Fig. 4.** Complementary behavior of neuronal and glial cells during seizure. Simultaneous field-potential and intracellular recordings from neuron and glial cell in neocortical area 7. The lateral distance between the neuron and glial cell is smaller (0.5 and 1 mm) between EEG and neuron. The fragment indicated by arrows is expanded below. The numbers indicate: PDS onset (1); depolarizing plateau (2); polyspike complexes (3); inter-PDS intervals (4). The averaged crosscorrelogram between neuron and glia indicates that neuronal depolarization precedes the depolarization of glial cell.

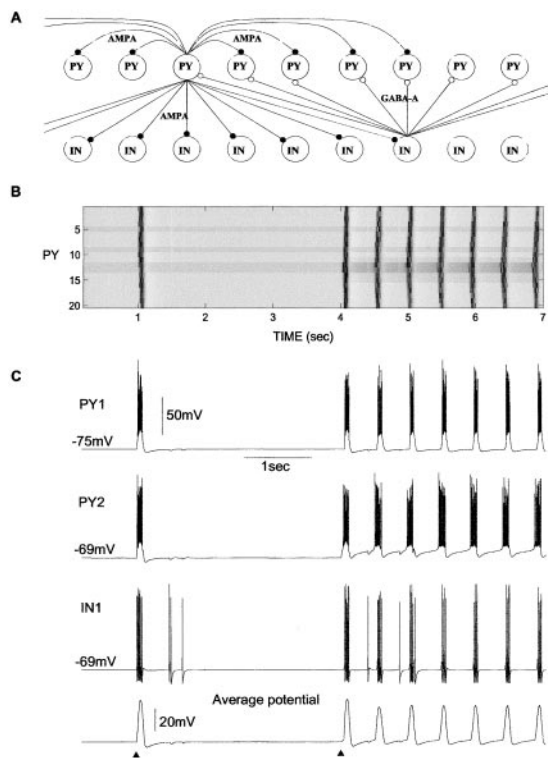


**Fig. 5.** A model of cortical self-sustained paroxysmal activity initiated by  $I_h$  and increased  $[K^+]_o$ . (A) Network geometry. (B) Two-dimensional plot of activity in the PY network. (C) The membrane potentials of two PY cells and one IN cell and average potential of all 20 PY cells. The silent state of the network was stable as illustrated by the experiment with external (AMPA-mediated excitatory postsynaptic potential) stimulation (first triangle). To model a local increase of  $[K^+]_o$ , the reversal potentials for  $K^+$  leak current and  $I_h$  as well as the maximal conductance for  $I_h$  were increased in the group of PY cells (second triangle). A single external stimulation initiated self-maintained 2-Hz oscillations. GABA<sub>A</sub>,  $\gamma$ -aminobutyric acid type A.

phasic depolarizing potentials during every paroxysmal cycle and maintained a steady depolarization throughout the seizures, reflecting an increased level of the  $[K^+]_o$  (26, 27). The onset of neuronal PDS was accompanied by a brief hyperpolarizing potential in the glial cell (Fig. 4). Thereafter, glial cells were depolarized, and during the neuronal plateau potential and polyspike complexes, the depolarization of glial cells reached maximum. Every fast-rising depolarizing event in neuronal polyspike complexes was reflected as a small hyperpolarization of the glial cell. The brief glial hyperpolarizations most likely reflected the field potential produced by simultaneous depolarization of neighboring neurons and recorded intracellularly in glial cells (28–30). The end of the paroxysmal cycle was characterized by a progressive repolarization of the glial cell (4 in Fig. 4), but its membrane potential reached the level seen prior to the seizure only at the complete cessation of the paroxysm. In neurons showing repolarizing potentials during the EEG wave, the maximal neuronal hyperpolarization was achieved immediately after the maximal depolarization of glial cells.

These results suggest that  $I_h$  of cortical neurons might mediate slow repolarizing potentials during EEG waves and thus might maintain paroxysmal activities under conditions of increased  $[K^+]_o$ . To support this hypothesis, we developed a computer model of self-sustained activity in a network model including layers of PY and IN cells. In the network displayed in Fig. 5,  $I_h$  was included in 4 of 20 PY neurons (cells 5, 9, 12, and 13). In the absence of external inputs, the network remained silent. An external excitatory postsynaptic potential (first triangle at Fig.

5C) applied to the small subset of PY neurons (cells 6–9) evoked bursts of spikes in these neurons. Through the lateral PY–PY connections, all the cortical neurons from the modeled network became involved in an active state. The activity lasted for 0.15–0.2 sec, maintained by  $I_{Na(P)}$  and high-threshold  $Ca^{2+}$  current, and was terminated primarily by  $I_{K(Ca)}$ , which caused an after-hyperpolarizing potential that lasted  $\approx 0.1$ –0.2 sec. The  $I_{K(Ca)}$ -dependent hyperpolarization activated  $I_h$  and could lead to rebound firing if the membrane potential repolarization was rapid (data not shown). However, if the repolarization was slow as a consequence of the slow deactivation of  $I_{K(Ca)}$ , the  $I_h$  became almost deactivated when PY cells were repolarized back to the resting potential. A weak  $I_h$ -dependent rebound depolarization was not sufficient to activate any other conductances that would support the future depolarization. In these “normal” conditions, the cortical network was not able to maintain oscillations, and thus it remained silent after a single period of activity.

To model the increase in the  $[K^+]_o$  in the paroxysmal foci, the reversal potential for  $I_{leak}$  was shifted up by  $\approx 5$  mV in the subset of five PY cells (cells 11–15), thus bringing their resting potential closer to the level of activation for  $I_{Na(P)}$ . Increase in the  $[K^+]_o$  affects both the reversal potential and the conductance underlying  $I_h$  (10, 31–33). In large neurons from layer V of cat sensorimotor cortex, increasing  $[K^+]_o$  from 3 to 12 mM increased the conductance by a factor of 1.8 (from 0.04 to 0.071  $\mu S$ ) at  $V_{hold} = -59$  mV and by factor of 3 (from 0.073 to 0.22  $\mu S$ ) at  $V_{hold} = -103$  mV (10). Elevated  $[K^+]_o$ , however, does not shift  $I_h$  activation curve (10, 33). A massive shift in amplitude of the  $I_h$  by  $[K^+]_o$  alterations suggests an additional regulatory binding site for  $K^+$  (34). To account for  $I_h$  up-regulation by  $[K^+]_o$ , in the model the maximal conductance for  $I_h$  and its reversal potential were also increased in the PY cells from the same set that had  $I_h$  (cells 12 and 13). In most simulations, the conductance increase was from 0.01 to 0.018  $\mu S$  (12); higher conductance values were tested also and led to stronger oscillations. These changes produced “abnormal” conditions in which previously weak  $I_h$ -dependent rebound depolarization became strong enough to activate  $I_{Na(P)}$  and initiate a new cycle of activity that propagated through the network (Fig. 5B and C). The onset of each paroxysmal cycle was always initiated in those two PY cells (12 and 13) in which the strength of  $I_h$  was increased. As in the case when activity was initiated by the external AMPA stimulation, the depolarization plateau was terminated after 0.1–0.2 sec and was followed by after-hyperpolarizing potential that increased  $I_h$  activation. We also tested a network in which only these two PY cells (cells 12 and 13; 10% of total population) had  $I_h$  and found similar oscillatory behavior with increase in the  $[K^+]_o$ . The exact frequency of the paroxysmal oscillations depended on the peak conductances for  $I_{K(Ca)}$ ,  $I_h$ , and the level of PY depolarization. Larger values of  $I_{K(Ca)}$  peak conductance produced a higher frequency of paroxysmal oscillations as  $I_h$  activation was increased by stronger membrane potential hyperpolarizations between depolarizing events (data not shown). Similar activity was found also in the network with 100 PY and 100 IN cells (with  $I_h$  included in 20 PY neurons).

## Discussion

Although several studies have suggested a cortical origin for SW paroxysmal activities (1, 23–25, 35), the intracortical mechanisms responsible for generation of paroxysmal oscillations remain uncertain. The EEG “wave” component of SW seizures is characterized by a dramatic increase in the intrinsic excitability of fast-spiking (presumably local inhibitory) neurons that contribute significantly to the generation of PDSs (36) and might mediate the high sensitivity of the neocortical network to synaptic volleys (37). Several factors are responsible for such an increase in sensitivity. First, the elevation of  $[K^+]_o$  increases cellular excitability (5–8). Under these conditions, the cortex is ready to respond to the synaptic inputs with paroxysmal discharges (37, 38). The second factor is an increase in synaptic

sensitivity. The next paroxysmal cycle originates during the neuronal silence that corresponds to the EEG wave in the SW complex. The short-term absence of synaptic activity increases the synaptic efficacy (14, 39). Because no neuron in the thalamocortical network fires action potentials during at least the early phase of the EEG wave component of cortically generated SW complexes, the source of activity probably is intrinsic. Indeed, intrinsic oscillation and resonance of single central neurons as well as their chemical and electrical synaptic contacts often lead to network oscillations (40). In our *in vivo* experiments, we found 20% of neurons that displayed a steady repolarization from hyperpolarized levels of the membrane potential. This repolarization, occurring at  $\approx -70$  mV and below, most likely is ascribable to an activation of  $I_h$  that produces postinhibitory excitation (41). Only cells with a clear depolarizing sag were included in the proportion reported here. There was also a population of neurons in which depolarizing sag was less prominent. Thus, in conditions of elevated  $[K^+]_o$  more neurons might reveal  $I_h$ . The presence of anomalous rectification was reported in a larger proportion of cortical neurons in other *in vivo* and *in vitro* studies (10–12, 42). The differences in the percentage of neurons revealing anomalous rectification could be caused by the state of anesthesia or to the concentration of specific ions in the extracellular bath *in vitro*. At least two factors are responsible for the appearance of slow-repolarizing potentials in only restricted populations of neocortical neurons. First, the  $I_h$  is not expressed equally in different subpopulations of neocortical neurons (41, 43, 44). Second, the  $I_h$  has to overwhelm the  $I_{K(Ca)}$  that is activated during paroxysmal activities (2).

Possible sources of hyperpolarization in paroxysmal foci include disfacilitation and  $I_{K(Ca)}$ . Neuronal hyperpolarization occurs when  $[K^+]_o$  is elevated, as estimated by intracellular recording from glial cells. An increase in  $[K^+]_o$  promotes  $I_h$  activation during neuronal hyperpolarization, which can lead to the onset of the next paroxysmal cycle. An increase in the level of maximum hyperpolarization in a neuron between depolarizing events during seizures (1) also would favor an increase of the effectiveness of  $I_h$ . This mechanism was confirmed by a computational model in which  $I_h$ ,  $I_{K(Ca)}$ , and  $I_{Na(per)}$  in pyramidal cells were sufficient to organize paroxysmal oscillations with a frequency of 2–3 Hz. These oscillations started when  $I_{K(leak)}$  and  $I_h$  reversal

potentials were depolarized and the maximal conductance for  $I_h$  was increased to model the increased  $[K^+]_o$  in paroxysmal foci (10). A single PY cell with these properties was sufficient to mediate activity in a whole cortical network of 40 neurons.

We cannot exclude the possibility that the  $T$  current also contributed to the generation of rebound overexcitation. *In vitro* studies have shown the presence of rebound  $Ca^{2+}$  spikes in cortical pyramidal neurons (45) and colocalization of the  $I_h$  and  $T$  current in cortical neurons (46). However, only very weak low-threshold  $Ca^{2+}$  spikes were obtained *in vivo* from voltages much more hyperpolarized than the most hyperpolarized membrane potential that occurs during spontaneous network operations (47). Also, the excursion of intracellular traces in which neurons fire spikes before the onset of PDS in the present study (see Fig. 4) does not suggest a major  $T$  current-mediated component. Thus, although other models of intracortical SW activity relied on the  $T$  current (48), we did not include the low-threshold  $Ca^{2+}$  current in the present study. Also, the increase of  $[K^+]_o$  is a consequence of paroxysmal firing, but in the present model elevated  $[K^+]_o$  also can trigger seizures. Our model predicts that paroxysmal discharges can propagate in athalamic animals, which is consistent with a previous study (35). Thus, we suggest that paroxysmal activity should be synchronized locally rather than globally across cortex, and we predict that blocking  $I_h$  pharmacologically or by genetic manipulation should increase the threshold for intracortical seizures.

Our model of paroxysmal activity in neocortex does not require that the thalamus be a source of excitation-triggering paroxysmal cycles in the thalamocortical system (49). Thalamic neurons often are hyperpolarized throughout the entire seizure and cannot contribute actively to paroxysmal cycles (23–25). The generation of intracortical paroxysmal activities may arise from a mosaic of intrinsic properties of cortical neurons and changes in extracellular ion concentrations.

We thank P. Giguère and D. Drolet for technical assistance. We also thank F. Greiner and S. Pandi-Perumal, who participated in some early experiments. This research was supported by National Institutes of Health Grant NS40522, Canadian Institutes of Health Research Grants MOP-36545 and MT-3689, Fonds de la Recherche en Santé du Québec, the Howard Hughes Medical Institute, and by the Human Frontier Science Program.

1. Steriade, M., Amzica, F., Neckelmann, D. & Timofeev, I. (1998) *J. Neurophysiol.* **80**, 1456–1479.
2. Alger, B. E. & Nicoll, R. A. (1980) *Science* **210**, 1122–1124.
3. Neckelmann, D., Amzica, F. & Steriade, M. (2000) *Neuroscience* **96**, 475–485.
4. Moody, W. J., Futamachi, K. J. & Prince, D. A. (1974) *Exp. Neurol.* **42**, 248–263.
5. Traynelis, S. F. & Dingledine, R. (1988) *J. Neurophysiol.* **59**, 259–276.
6. McNamara, J. O. (1994) *J. Neurosci.* **14**, 3413–3425.
7. Jensen, M. S., Azouz, R. & Yaari, Y. (1994) *J. Neurophysiol.* **71**, 831–839.
8. Jensen, M. S. & Yaari, Y. (1997) *J. Neurophysiol.* **77**, 1224–1233.
9. Timofeev, I., Grenier, F., Bazhenov, M., Sejnowski, T. J. & Steriade, M. (2000) *Cereb. Cortex* **10**, 1185–1199.
10. Spain, W. J., Schwindt, P. C. & Crill, W. E. (1987) *J. Neurophysiol.* **57**, 1555–1576.
11. Hutcheon, B., Miura, R. M. & Puil, E. (1996) *J. Neurophysiol.* **76**, 683–697.
12. Hutcheon, B., Miura, R. M. & Puil, E. (1996) *J. Neurophysiol.* **76**, 698–714.
13. Tsodyks, M. V. & Markram, H. (1997) *Proc. Natl. Acad. Sci. USA* **94**, 719–723.
14. Galarreta, M. & Hestrin, S. (1998) *Nat. Neurosci.* **1**, 587–594.
15. Bazhenov, M., Timofeev, I., Steriade, M. & Sejnowski, T. J. (1998) *J. Neurosci.* **18**, 6444–6465.
16. Mainen, Z. F. & Sejnowski, T. J. (1996) *Nature (London)* **382**, 363–366.
17. Alzheimer, C., Schwindt, P. C. & Crill, W. E. (1993) *J. Neurosci.* **13**, 660–673.
18. Kay, A. R., Sugimori, M. & Llinás, R. R. (1998) *J. Neurophysiol.* **80**, 1167–1179.
19. Connors, B. W. & Gutnick, M. J. (1990) *Trends Neurosci.* **13**, 99–104.
20. Gray, C. M. & McCormick, D. A. (1996) *Science* **274**, 109–113.
21. Steriade, M., Timofeev, I., Dürmüller, N. & Grenier, F. (1998) *J. Neurophysiol.* **79**, 483–490.
22. Pape, H. C. (1996) *Annu. Rev. Physiol.* **58**, 299–327.
23. Steriade, M. & Contreras, D. (1995) *J. Neurosci.* **15**, 623–642.
24. Pinault, D., Leresche, N., Charpier, S., Deniau, J. M., Marescaux, C., Vergnes, M. & Crunelli, V. (1998) *J. Physiol. (London)* **509**, 449–456.
25. Timofeev, I., Grenier, F. & Steriade, M. (1998) *J. Neurophysiol.* **80**, 1495–1513.
26. Pedley, T. A., Fisher, R. S., Futamachi, K. J. & Prince, D. A. (1976) *Fed. Proc.* **35**, 1254–1259.
27. Futamachi, K. J. & Pedley, T. A. (1976) *Brain Res.* **109**, 311–322.
28. Amzica, F. & Steriade, M. (2000) *J. Neurosci.* **20**, 6648–6665.
29. Taylor, C. P. & Dudek, F. E. (1984) *J. Neurophysiol.* **52**, 143–155.
30. Dudek, F. E., Yasumura, T. & Rash, J. E. (1998) *Cell Biol. Int.* **22**, 793–805.
31. Solomon, J. S. & Nerbonne, J. M. (1993) *J. Physiol. (London)* **462**, 393–420.
32. McCormick, D. A. & Pape, H. C. (1990) *J. Physiol. (London)* **431**, 291–318.
33. Hestrin, S. (1987) *J. Physiol. (London)* **390**, 319–333.
34. Kilb, W. & Luhmann, H. J. (2000) *J. Neurophysiol.* **84**, 1681–1691.
35. Steriade, M. & Contreras, D. (1998) *J. Neurophysiol.* **80**, 1439–1455.
36. Timofeev, I., Grenier, F. & Steriade, M. (2002) *Neuroscience*, in press.
37. Steriade, M. & Amzica, F. (1999) *J. Neurophysiol.* **82**, 3108–3122.
38. Traub, R. D. & Dingledine, R. (1990) *J. Neurophysiol.* **64**, 1009–1018.
39. Abbott, L. F., Varela, J. A., Sen, K. & Nelson, S. B. (1997) *Science* **275**, 220–224.
40. Llinás, R. R. (1988) *Science* **242**, 1654–1664.
41. Spain, W. J., Schwindt, P. C. & Crill, W. E. (1991) *J. Physiol. (London)* **434**, 609–626.
42. Baranyi, A., Szenté, M. B. & Woody, C. D. (1993) *J. Neurophysiol.* **69**, 1864–1879.
43. Spain, W. J., Schwindt, P. C. & Crill, W. E. (1991) *J. Physiol. (London)* **434**, 591–607.
44. Spain, W. J. (1994) *J. Neurophysiol.* **72**, 1925–1937.
45. de la Peña, E. & Geijo-Barrientos, E. (1996) *J. Neurosci.* **16**, 5301–5311.
46. Foehring, R. C. & Waters, R. S. (1991) *Neurosci. Lett.* **124**, 17–21.
47. Paré, D. & Lang, E. J. (1998) *Eur. J. Neurosci.* **10**, 3164–3170.
48. Destexhe, A., Contreras, D. & Steriade, M. (2001) *Neurocomputing* **38–40**, 555–563.
49. Destexhe, A. (1998) *J. Neurosci.* **18**, 9099–9111.